Nigerian Research Journal of Engineering and Environmental Sciences 6(1) 2021 pp. 370-386

Nigerian Research Journal of Engineering and Environmental Sciences
Journal homepage: www.rjees.com

Original Research Article

Application of Active Filters in Power Systems

***[1]Onah, A.J., [2]Ezema, E.E. and [3]Uzodife, N.A.**

[1]Department of Electrical/Electronic Engineering, College of Engineering and Engineering Technology, Michael Okpara University of Agriculture, Umudike, Abia State, Nigeria.
[2]Department of Electrical/Electronic Engineering, School of Engineering, Enugu State Polytechnic, Iwollo, Enugu State, Nigeria.
[3]Department of Electrical Engineering, Federal Ministry of Works and Housing, Abuja, Nigeria.
*aniagbosoonah@yahoo.com

ARTICLE INFORMATION

Article history:
Received 19 Dec, 2020
Revised 23 Apr, 2021
Accepted 01 May, 2021
Available online 30 Jun, 2021

Keywords:
Non-linear loads
Current harmonics
Reactive power
Power factor
Active filter

ABSTRACT

This paper is intended to show how current harmonics are generated by some nonlinear loads, and how these harmonics can be suppressed. Majority of loads such as induction motors, battery chargers, static converters, light fittings, arc furnaces, transformers, cables, and transmission lines draw both sinusoidal currents and currents which are multiples of the supply frequency, commonly called harmonics. These harmonics pollute the AC mains resulting in poor quality power supply, which is detrimental to many sensitive loads. This paper shows how an active filter (AF) can be used to filter the harmonics in the supply current so as to produce near-sinusoidal current. The paper describes the operation of both the non-linear load and the active filter. The performance equations are derived, and the characteristics obtained. The phase-controlled rectifier is a major cause of harmonic pollution in the AC system network. As an example of nonlinear load, the three-phase, full-wave controlled rectifier was examined. The principle of operation of the rectifier was described, the input equations derived, and the distorted input current characteristic shown. Application of the active filter (AF) to minimize these harmonics follows. The application of active filter results in sinusoidal currents, and consequently reduction in total harmonic distortion (THD) and improvement in system power factor.

1. INTRODUCTION

The total demand on the supply for a nonlinear load like the phase-controlled rectifier is called apparent power, which is the vector sum of both active and reactive components of power. The active power is the result of the sinusoidal current drawn by the load, while the harmonics give rise to the reactive power. The

active power produces mechanical power and heat. The reactive power magnetizes the cores of electrical machines like transformers, generators etc. However, the flow of reactive power in electrical networks has the following adverse effects: low power factor, voltage sag, network losses in the form of I^2R (where I is the line current and R line resistance). Consequently, available network capacity is reduced, and generation and transmission equipment will need to be enhanced. In three-phase networks, these harmonics cause unbalance and excessive neutral currents. Harmonics give rise to interference in nearby communication networks and disturbance to other consumers. In electric motor drives, they cause torque pulsations and cogging (Emanuel and Yang, 1993). In networks feeding harmonic-current-producing nonlinear loads, filters are used to prevent harmonic currents from entering the utility system.

Power factor is the ratio of active power to apparent power, and is given by $\cos\theta_1$ (θ_1 is the angle between the fundamental components of voltage and current). When the current lags the voltage in phase rotation, the load is drawing reactive power from the source and power factor is said to be lagging, but when current leads the voltage, reactive power is being returned to the source and the power factor is said to be leading. This power factor is known as displacement power factor (DPF) because it is based on the fundamental quantities of voltage and current. 'true power factor' is the power factor involving the effect of harmonic distortion on the voltage and current waveforms of a load (Bose, 2000). The aim of this paper is to show how harmonic distortion is caused by nonlinear load in the system as well as how this harmonic distortion can be reduced.

2. MATERIALS AND METHODS

2.1. Generation of Harmonics (Nonlinear Load)

As nonlinear load, the phase-controlled rectifier is the major source of supply of harmonics and cause of poor power factor in ac mains (Katic and Graovac, 2002). The controlled six-pulse three-phase converter is shown in Figure 1 (Rim et al, 1995; Bose, 2000). Motor speed control systems, electromechanical and electrometallurgical processes, magnet power supplies, DC transmission, portable hand tools, uninterruptible power supplies, and closed-loop control systems are some of the industrial applications of three-phase rectifiers (Rashid, 1993; Katic and Graovac, 2002). They provide two-quadrant operation - output voltage can have positive or negative polarity. Due to its bidirectional power-transfer capability (i.e. the rectifier can also be operated as an inverter, whereby energy is returned to the source.), energy recovery is possible when the motors are braking in traction drives (Qiao and Smeldley, 2002).

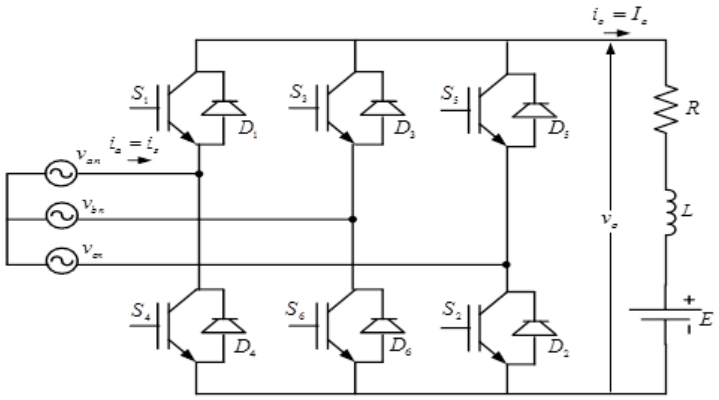

Figure 1: Six-pulse fully controlled three-phase rectifier

The three-phase bridge rectifier, with six switches, produces six pulses of the output voltage per cycle; and better output voltage waveform than the single-phase bridge (Qiao and Smeldley, 2002). So, the desirable continuous current condition is more readily achieved. With current continuity, current ripples in a motor, and hence torque ripples are suppressed (Allmeling, 2004). When a gate signal is applied while the switch

is forward biased, conduction starts. Switches are fired in the sequence they are numbered, with a phase difference of 60°. Only two suitable switches must conduct at the same time for current to flow from the supply side to the load side – one odd-numbered and one even-numbered) (Marafao et al., 2004). Turning on of an odd-numbered switch, means that the previously conducting odd-numbered switch has been commutated. This also applies to the even-numbered switches, so that the conduction angle for each switch is 120° of the supply frequency.

2.2. Rectifier Input Quantities

The three source phase voltages, v_{an}, v_{bn}, and v_{cn} combine to produce the line-to-line voltages v_{ab}, v_{bc}, and v_{ca}. The conduction of any pair of switches is decided by the positive maximum of a line-to-line voltage, which appears as an output voltage v_o across the load when the appropriate switches conduct. For example, when the line voltage v_{ab} is dominantly positive at $\omega t = \pi/3$, S_1 and S_6 conduct simultaneously and v_{ab} appears across the load. The firing sequence of the switches, and the voltage applied across the load are shown in Table 1.

Table 1: Firing sequence of the switches, and the voltage applied across the load

Interval	Switches conducting	Voltage applied to load
$\left(\pi/3 + \alpha\right) \le \omega t \le \left(2\pi/3 + \alpha\right)$	S_6, S_1	v_{ab}
$\left(2\pi/3 + \alpha\right) \le \omega t \le \left(\pi + \alpha\right)$	S_1, S_2	v_{ac}
$\left(\pi + \alpha\right) \le \omega t \le \left(4\pi/3 + \alpha\right)$	S_2, S_3	v_{bc}
$\left(4\pi/3 + \alpha\right) \le \omega t \le \left(5\pi/3 + \alpha\right)$	S_3, S_4	v_{ba}
$\left(5\pi/3 + \alpha\right) \le \omega t \le \left(2\pi + \alpha\right)$	S_4, S_5	v_{ca}
$\left(2\pi + \alpha\right) \le \omega t \le \left(7\pi/3 + \alpha\right)$	S_5, S_6	v_{cb}

The line-to-neutral voltages are defined as:

$$v_{an} = V_m \sin \omega t \tag{1}$$

$$v_{bn} = V_m \sin\left(\omega t - \frac{2\pi}{3}\right) \tag{2}$$

$$v_{cn} = V_m \sin\left(\omega t + \frac{2\pi}{3}\right) \tag{3}$$

The line-to-line voltages are defined as:

$$v_{ab} = V_m \sin \omega t \tag{4}$$

$$v_{ac} = V_m \sin\left(\omega t - \frac{\pi}{3}\right) \tag{5}$$

$$v_{bc} = V_m \sin\left(\omega t - \frac{2\pi}{3}\right) \tag{6}$$

$$v_{ba} = V_m \sin\left(\omega t - \pi\right) \tag{7}$$

$$v_{ca} = V_m \sin\left(\omega t + \frac{2\pi}{3}\right) \tag{8}$$

$$v_{cb} = V_m \sin\left(\omega t + \frac{\pi}{3}\right) \tag{9}$$

The instantaneous input current of a phase of the three-phase rectifier can be expressed in Fourier series as:

$$i_s(t) = \frac{a_0}{2} + \sum_{n=1\ldots}^{\infty}\left(a_n \cos n\omega t + b_n \sin n\omega t\right) \tag{10}$$

The Fourier coefficients a_o, and, a_n b_n can be obtained as follows:

$\frac{a_0}{2}$ is the dc component of the input current, I_{dc}.

$$\frac{a_0}{2} = \frac{1}{2\pi}\int_0^{2\pi} i_s(t)d\omega t = \frac{1}{2\pi}\left[\int_{\frac{\pi}{3}+\alpha}^{\pi+\alpha} I_a d\omega t - \int_{\frac{4\pi}{3}+\alpha}^{2\pi+\alpha} I_a d\omega t\right] = 0 \tag{11}$$

I_a is the average value of the output current

$$a_n = \frac{1}{\pi}\int_0^{2\pi} i_s(t)\cos n\omega t\, d(\omega t) = \frac{1}{\pi}\left[\int_{\frac{\pi}{3}+\alpha}^{\pi+\alpha} I_a \cos n\omega t\, d(\omega t) - \int_{\frac{4\pi}{3}+\alpha}^{2\pi+\alpha} I_a \cos n\omega t\, d(\omega t)\right] \tag{12}$$

$$a_n = \frac{4I_a}{n\pi}\sin\frac{n\pi}{2}\sin\frac{n\pi}{3}\sin\left(\frac{7n\pi}{6} + n\alpha\right)$$

$$b_n = \frac{1}{\pi}\int_0^{2\pi} i_s(t)\sin n\omega t\, d(\omega t) = \frac{1}{\pi}\left[\int_{\frac{\pi}{3}+\alpha}^{\pi+\alpha} I_a \sin n\omega t\, d(\omega t) - \int_{\frac{4\pi}{3}+\alpha}^{2\pi+\alpha} I_a \sin n\omega t\, d(\omega t)\right] \tag{13}$$

$$b_n = -\frac{4I_a}{n\pi}\sin\frac{n\pi}{2}\sin\frac{n\pi}{3}\cos\left(\frac{7n\pi}{6} + n\alpha\right)$$

Combination of Equations 11 to 13, with Equation 10 yields Equation (14).

$$i_s(t) = \sum_{n=1\ldots}^{\infty} C_n \sin\left(n\omega t - n\alpha\right) = \sum_{n=1\ldots}^{\infty} C_n \sin\left(n\omega t + \theta_n\right) \tag{14}$$

$$C_n = \sqrt{a_n^2 + b_n^2} = \frac{4I_a}{n\pi}\sin\frac{n\pi}{2}\sin\frac{n\pi}{3} \tag{15}$$

$$\theta_n = \tan^{-1}\frac{a_n}{b_n} = -n\alpha$$

When n=1, $\theta_1 = -\alpha$

The rms value of the n^{th} harmonic input current is:

$$I_{sn} = \frac{C_n}{\sqrt{2}} = \frac{2\sqrt{2}\, I_a}{n\pi} \sin\frac{n\pi}{2} \sin\frac{n\pi}{3} \tag{16}$$

The rms value of the fundamental current is:

$$I_{s1} = \frac{2\sqrt{2}\, I_a}{\pi} x \frac{\sqrt{3}}{2} = \frac{\sqrt{6}\, I_a}{\pi} \tag{17}$$

The rms value of the input current is given as:

$$I_s = \left[\sum_{n=1}^{\infty} I_{sn}^2\right]^{\frac{1}{2}} \tag{18}$$

The total harmonic distortion (THD) of the input current is given by:

$$THD = \left[\left(\frac{I_s}{I_{s1}}\right)^2 - 1\right]^{\frac{1}{2}} \tag{19}$$

The power factor (PF) is given by:

$$PF = \frac{I_{s1}}{I_s} \cos\theta_1 = \frac{Is_1}{I_s} \cos\alpha \tag{20}$$

θ_1 is the angle between the fundamental components of voltage and current.

2.3. Reduction of Harmonics

Figure 2 shows a system comprising of the AC mains, active filter, and the non-linear load (the rectifier). The various currents flowing in the system are shown. The current drawn by the nonlinear load consists of a fundamental-frequency component i_{S_1} and a distortion component, known as harmonics. The load current is sensed and filtered to provide a signal proportional to the distortion component. A switch-mode DC-to-AC converter (active filter) is operated to deliver the distortion component to the utility. Thus, in an ideal case, the harmonics in the utility current are eliminated.

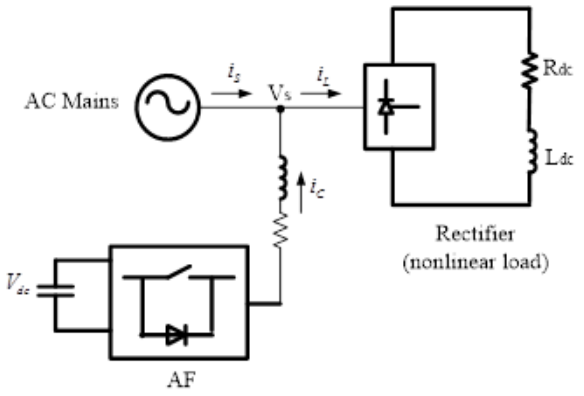

Figure 2: Voltage-fed-type AF connected to a non-linear load (rectifier)

Extensive research has developed active filters (AF) that are relatively lighter in weight, cheaper and more efficient (Nastran et al., 1994). Active filters prevent harmonic currents from entering the utility system, if harmonic-current-producing nonlinear loads are being supplied by the utility; thus producing sinusoidal currents at near-unity power factor. Active filters are inverter circuits, comprising of active devices that can be controlled so as to act as harmonic current or voltage generators. Different topologies and control techniques have been developed. One of the commonest topology in use is the voltage-source inverter shown in Figure 3. It is a three-phase, 6-pulse, full-bridge voltage source inverter (DC-to-AC Converter). It can be used as an active filter (AF). The inverter consists of six active switches with anti-parallel diode connected across each of the active switches (S_1, S_2, S_3, S_4, S_5, and S_6). The circuit produces a three-phase ac output voltage from a DC input, V_{dc}. Switch pair, S_1, S_4 close and open opposite of each other. They must not close or open at the same time so as not to cause short-circuit. So also are the pairs, S_2, S_5 and S_3, S_6.

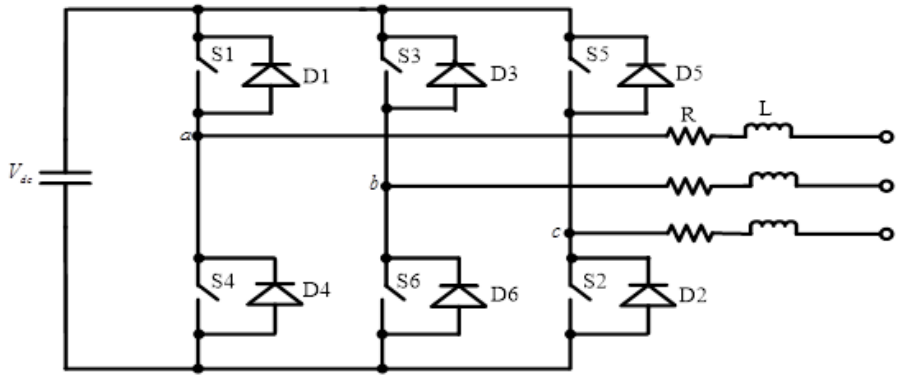

Figure 3: Three-phase voltage source inverter

3. RESULTS AND DISCUSSION

3.1. Principles of Operation

The working principles of the major devices employed in this paper are explained thus.

3.1.1. Three-phase controlled rectifier (nonlinear load)

Equations (4) – (9) are plotted as shown in Figure 4. These are the waveforms of the line-to-line voltages. It can be noticed in Figure 4 that at $\omega t = \pi/3$ the value of v_{ab} is higher than any of the other five source voltages. The gate signal is applied to switches S_1 and S_6 during the interval $\left(\pi/3 + \alpha\right) \leq \omega t \leq \left(2\pi/3 + \alpha\right)$ and the voltage v_{ab} appears across the load. At $\left(2\pi/3 + \alpha\right)$, the dominant line voltage is v_{ac} and S_2 is turned on as S_6 is reversed biased. So S_1 conducts for another 60° and goes off at $\left(\pi + \alpha\right)$, and S_3 comes on, and line current becomes zero. S_2 and S_3 remain the path for the load current until $\omega t = \left(4\pi/3 + \alpha\right)$, when line voltage v_{ba} dominates, and S_2 is turned off, while S_4 is fired. The load current then flows through S_4. Meanwhile supply current is restored in phase 'a' in the opposite direction. At $\omega t = \left(5\pi/3 + \alpha\right)$, v_{ca} is dominantly positive and S_3 is switched off by firing S_5. The supply line current and load current flow through S_5 and S_4, until at $\omega t = \left(2\pi + \alpha\right)$ when S_6 is fired and S_4 is turned off.

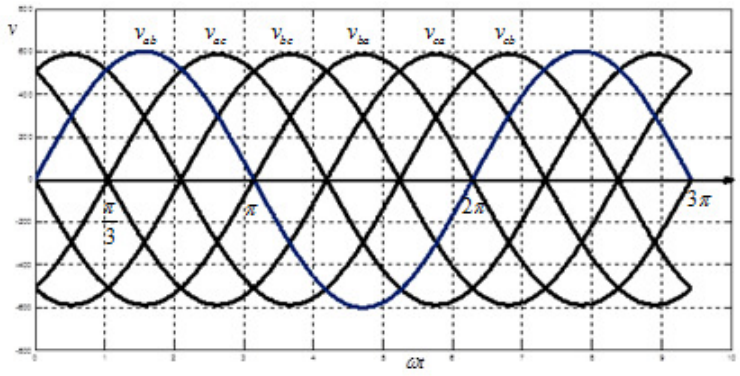

Figure 4: Input line-to-line voltage waveforms

The waveform of the supply-side voltage, v_S and current i_s for $\alpha = 75^o$ are shown in Figure 5, which is generated from Equation (10) or (14). It is the pulsed, fluctuating, non-sinusoidal current i_s drawn by the rectifier from the utility grid; that is the rectifier input current that causes harmonic pollution, poor power factor, voltage drop across the grid impedance in the vicinity, and distorted voltage waveform (Dubey, 1989; Fitzgerald et al., 2003; Maheshwari et al., 2013; Chen et al., 2014). i_{s1} is fundamental component, and $I_a = I_o$. I_o is the average output current.

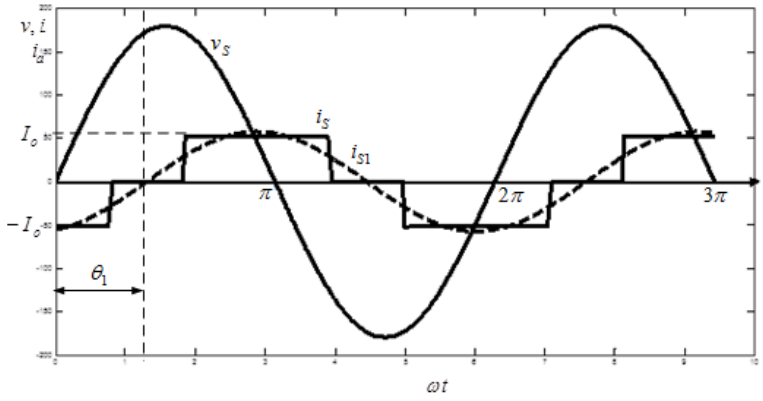

Figure 5: Waveform of supply line current (i_s), for $\alpha = 75^o$

The *THD* of the input current is:

$$THD = \left[\left(\frac{I_s}{I_{s1}}\right)^2 - 1\right]^{\frac{1}{2}} = \left[\left(\frac{3609.5}{3291.9}\right) - 1\right]^{\frac{1}{2}} = 0.3106 = 31.06\%$$

Note that I_s is generated from Equation 18 for $1 \leq n \leq 2000$ and $I_{s1} = I_s$ for n = 1.

The power factor of the system is:

$$PF = \frac{I_{s1}}{I_s}\cos\theta_1 = \frac{57.375}{60.079}x\cos 75^o = 0.25$$

Rectifiers that can operate at unity power factor, and generate sinusoidal currents are needed for inverter-based industrial loads (Singh et al., 1999). Some standards for harmonic distortion level have been

established, for utility industries to follow so as to maintain good power quality (Nastran et al., 1994; Srianthumrong et al. 2002). In other to meet the requirements of these standards, input filter may be used to suppress the harmonics.

3.1.2. Three-phase voltage source inverter

The switches in Figure 3 (three-phase voltage source inverter) are closed and opened in the modes, I, II, III, IV, V and VI shown in Figure 6 to produce line-to-line output voltages (v_{ab} , v_{bc} , v_{ca}) also shown in Figure 6. Each mode consists of three switches conducting at the same time. For the switches to conduct, gate signals, g_1, g_2, g_3, g_4, g_5 and g_6 are applied to switches S_1, S_2, S_3, S_4, S_5 and S_6 respectively.

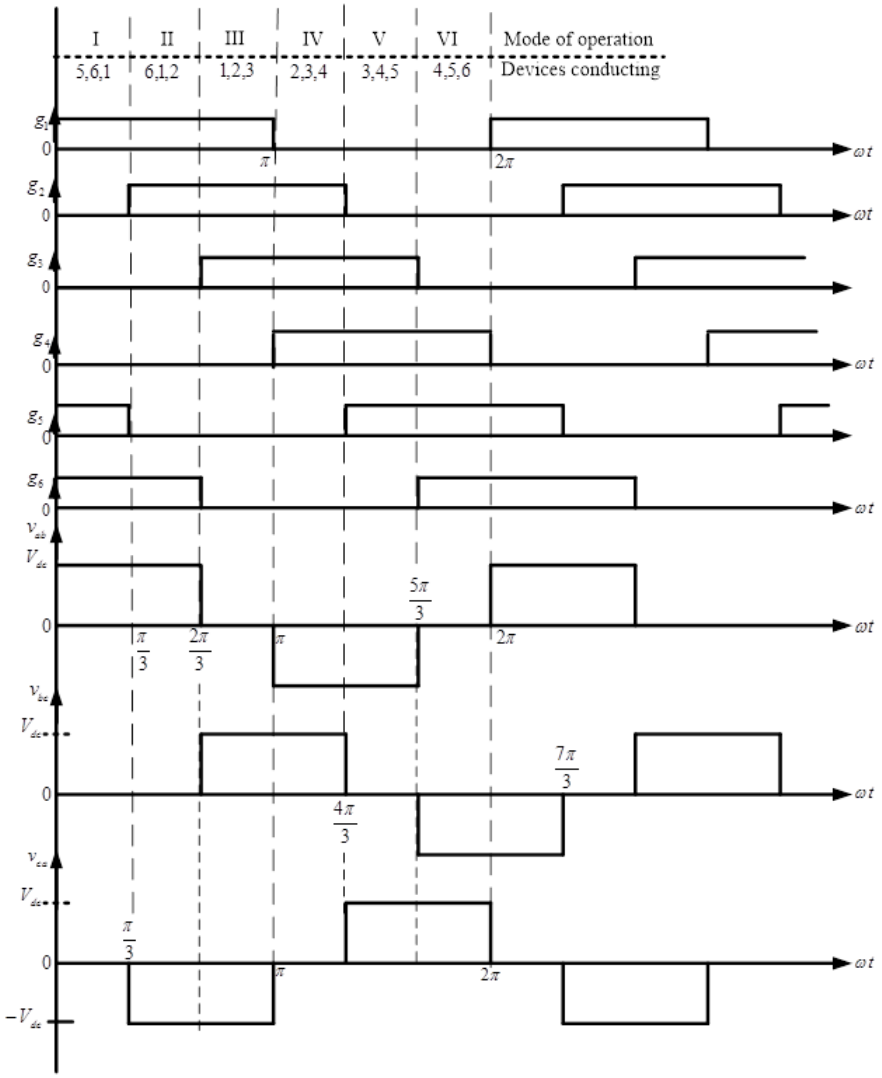

Figure 6 Switching modes and line-to-line output voltages of 3-phase inverter

The inverter load, Z connected in star is shown in Figure 7, and it gives the modes of operation in Figure 8.

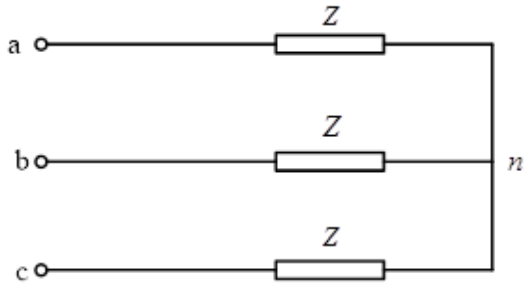

Figure 7 Star-connected load

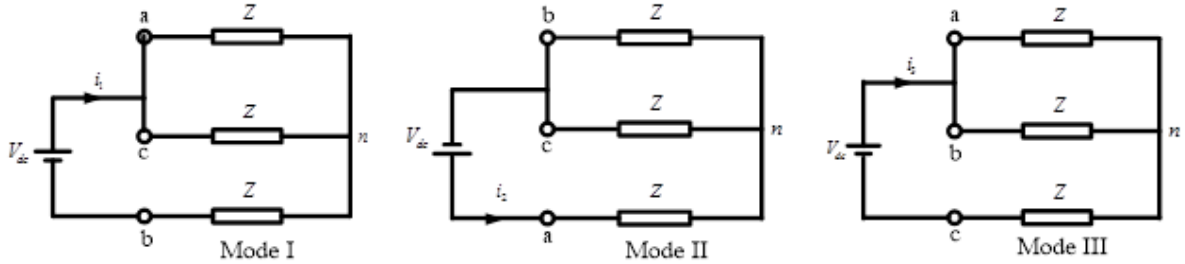

Figure 8 Modes of operation

When Switches S_5, S_6, S_1 conduct during the interval $0 \le \omega t < \frac{\pi}{3}$ (mode I), then:

$$Z_{eq} = \frac{Z}{2} + Z = \frac{3Z}{2}\ ,\ i_1 = \frac{V_{dc}}{Z_{eq}} = \frac{V_{dc}}{3Z/2} = \frac{2V_{dc}}{3Z},\ \ v_{an} = v_{cn} = \frac{Z}{2}\,x\,i_1 = \frac{Z}{2}x\frac{2V_{dc}}{3Z} = \frac{V_{dc}}{3},$$
$$v_{bn} = Z\,x - i_1 = Z\,x - \frac{2V_{dc}}{3Z} = -\frac{2V_{dc}}{3} \tag{21}$$

When Switches S_6, S_1, S_2 conduct during the interval $\frac{\pi}{3} \le \omega t < \frac{2\pi}{3}$ (mode II), then:

$$Z_{eq} = \frac{Z}{2} + Z = \frac{3Z}{2}\ ,\ i_2 = \frac{V_{dc}}{Z_{eq}} = \frac{V_{dc}}{3Z/2} = \frac{2V_{dc}}{3Z},$$
$$v_{an} = Z\,x\,i_2 = Z\,x\frac{2V_{dc}}{3Z} = \frac{2V_{dc}}{3},\ \ v_{bn} = v_{cn} = -i_2\,x\frac{Z}{2} = -\frac{2V_{dc}}{3Z}\,x\frac{Z}{2} = -\frac{V_{dc}}{3} \tag{22}$$

When Switches S_1, S_2, S_3 conduct during the interval $\frac{2\pi}{3} \le \omega t < \pi$ (mode III), then:

$$Z_{eq} = \frac{Z}{2} + Z = \frac{3Z}{2}\ ,\ i_3 = \frac{V_{dc}}{Z_{eq}} = \frac{V_{dc}}{3Z/2} = \frac{2V_{dc}}{3Z},$$
$$v_{an} = v_{bn} = \frac{Z}{2}\,x\,i_3 = \frac{Z}{2}x\frac{2V_{dc}}{3Z} = \frac{V_{dc}}{3},\quad v_{cn} = -i_3\,xZ = -\frac{2V_{dc}}{3Z}\,xZ = -\frac{2V_{dc}}{3} \tag{23}$$

Equations for the other modes of operation can be obtained similarly.

Thus, the star-connected load gives rise to the line-to-neutral voltages v_{an}, v_{bn} and v_{cn} – (Equations 21 to 23). These equations are plotted as shown in Fig. 9.

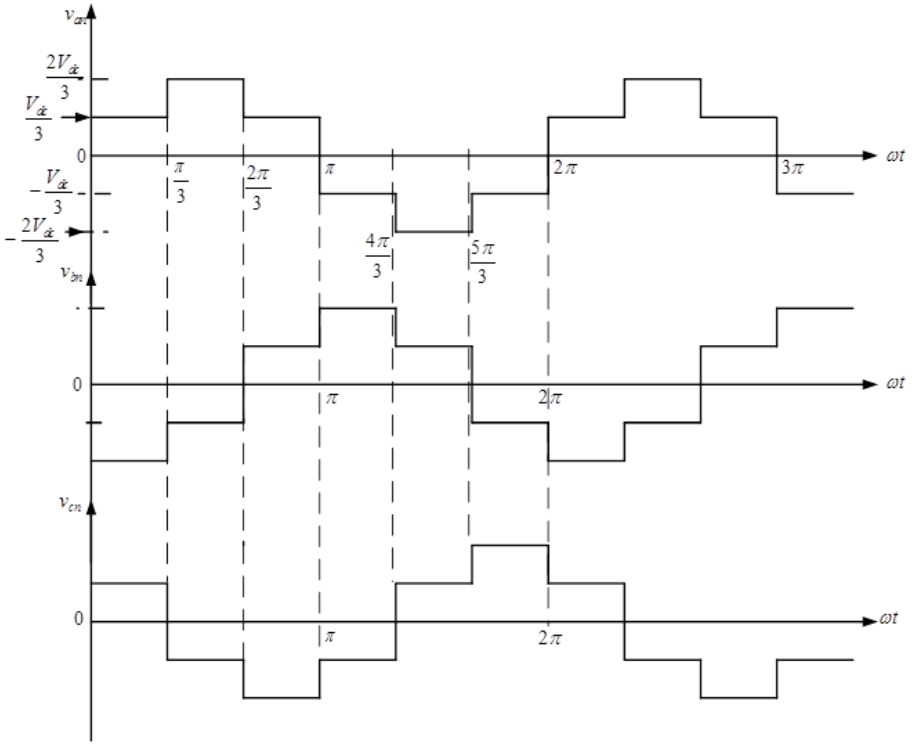

Figure 9: Line-to-neutral voltage patterns of three-phase inverter

The output voltages of the three-phase inverter can be analyzed using Fourier series. Such analysis helps to validate the voltage waveforms obtained in Figure 6 and Figure 9. In other words, Figure 6 and Figure 9 can be verified by Fourier series analysis.

Thus the line-to-line voltage of the three-phase inverter can be stated as:

$$V_{ab} = \frac{a_0}{2} + \sum_{n=1...}^{\infty} \{a_n \cos n\omega t + b_n \sin n\omega t\} \tag{24}$$

The Fourier coefficients a_0, a_n, and b_n can be found from Figure 6 as:

$$a_0 = \frac{1}{\pi}\int_0^{2\pi/3} V_{dc}\, d\omega t - \int_{\pi}^{5\pi/3} V_{dc}\, d\omega t = 0 \tag{25}$$

$$a_n = \frac{1}{\pi}\int_0^{2\pi/3} V_{dc} \cos n\omega t d\omega t - \int_{\pi}^{5\pi/3} V_{dc} \cos n\omega t d\omega t = \frac{V_{dc}}{n\pi}\left[\sin\frac{2n\pi}{3} - \sin\frac{5n\pi}{3} + \sin n\pi\right] \tag{26}$$

$$b_n = \frac{1}{\pi}\int_0^{2\pi/3} V_{dc}\sin n\omega t d\omega t - \int_{\pi}^{5\pi/3} V_{dc}\sin n\omega t d\omega t = \frac{V_{dc}}{n\pi}\left[1+\cos\frac{5n\pi}{3}-\cos\frac{2n\pi}{3}-\cos n\pi\right] \quad (27)$$

Equations (25), (26) and (27) combined resulted in Equation (28):

$$v_{ab} = \sum_{1,3,5...}^{\infty}\frac{4V_{dc}}{n\pi}\cos\left(\frac{n\pi}{6}\right)\sin n\left(\omega t+\frac{\pi}{6}\right) \quad (28)$$

for n odd (n=1,3,5,7, …)

The voltage v_{bc} lags v_{ab} by 120º and v_{ca} lags v_{bc} by 120º. Therefore:

$$v_{bc} = \sum_{1,3,5...}^{\infty}\frac{4V_{dc}}{n\pi}\cos\left(\frac{n\pi}{6}\right)\sin n\left(\omega t-\frac{\pi}{2}\right) \quad (29)$$

$$v_{ca} = \sum_{1,3,5...}^{\infty}\frac{4V_{dc}}{n\pi}\cos\left(\frac{n\pi}{6}\right)\sin n\left(\omega t-\frac{7\pi}{6}\right) \quad (30)$$

Figure 10 is the line voltage waveforms generated from Equations (28) to (30).

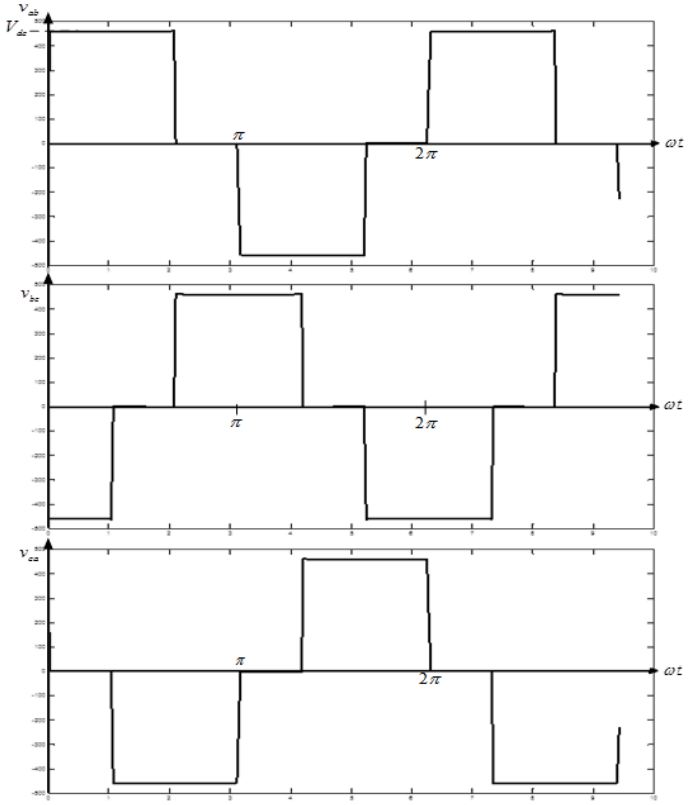

Figure 10: Line-to-line voltage waveforms of three-phase inverter

It can be observed that the line-to-line voltage waveforms shown in Figure 6 and Figure 10 are similar. These waveforms have square shape, and so this inverter is also referred to as square-wave inverter.

The line-to-neutral output voltage of Figure 9 can be expressed in Fourier series as:

$$v_{an} = \frac{a_0}{2} + \sum_{n=1\ldots}^{\infty} \{a_n \cos n\omega t + b_n \sin n\omega t\} \tag{31}$$

The Fourier coefficients can be found from Figure 9 as follows:

$$a_o = \frac{1}{\pi}\left[\int_0^{\pi/3} V_{dc}\, d\omega t + \int_{\pi/3}^{2\pi/3} V_{dc}\, d\omega t + \int_{2\pi/3}^{\pi} V_{dc}\, d\omega t + \int_{\pi}^{4\pi/3} V_{dc}\, d\omega t\right] = 0 \tag{32}$$

$$a_n = \frac{1}{\pi}\left\{\frac{V_{dc}}{3}\int_0^{\pi/3} \cos n\omega t d\omega t + \frac{2V_{dc}}{\pi}\int_{\pi/3}^{2\pi/3} \cos n\omega t d\omega t + \frac{V_{dc}}{3}\int_{2\pi/3}^{\pi} \cos n\omega t d\omega t - \frac{V_{dc}}{3}\int_{\pi}^{4\pi/3} \cos n\omega t d\omega t - \frac{2V_{dc}}{3}\int_{4\pi/3}^{5\pi/3} \cos n\omega t d\omega t - \frac{V_{dc}}{3}\int_{5\pi/3}^{2\pi} \cos n\omega t d\omega t\right\} \tag{33}$$

$$b_n = \frac{1}{\pi}\left\{\frac{V_{dc}}{3}\int_0^{\pi/3} \sin n\omega t d\omega t + \frac{2V_{dc}}{\pi}\int_{\pi/3}^{2\pi/3} \sin n\omega t d\omega t + \frac{V_{dc}}{3}\int_{2\pi/3}^{\pi} \sin n\omega t d\omega t - \frac{V_{dc}}{3}\int_{\pi}^{4\pi/3} \sin n\omega t d\omega t - \frac{2V_{dc}}{3}\int_{4\pi/3}^{5\pi/3} \sin n\omega t d\omega t - \frac{V_{dc}}{3}\int_{5\pi/3}^{2\pi} \sin n\omega t d\omega t\right\} \tag{34}$$

When Equations (32) to (34) are combined, Equation (35) is obtained:

$$v_{an} = \sum_{n=6p\pm1}^{\infty} \frac{2V_{dc}}{n\pi} \sin n\omega t \tag{35}$$

$$v_{bn} = \sum_{n=6p\pm1}^{\infty} \frac{2V_{dc}}{n\pi} \sin n\left(\omega t - \frac{2\pi}{3}\right) \tag{36}$$

$$v_{cn} = \sum_{n=6p\pm1}^{\infty} \frac{2V_{dc}}{n\pi} \sin n\left(\omega t - \frac{4\pi}{3}\right) \tag{37}$$

v_{bn} and v_{cn} lag v_{an} by 120_o and 240^o degrees respectively

$p = 0, 1, 2...$

For star-connected load, the current can be found to be:

$$i_a = \frac{v_{an}}{Z_n \angle \theta} = \sum_{n=6p\pm1}^{\infty} \frac{2V_{dc}}{n\pi Z_n} \sin(n\omega t - \theta_n) \tag{38}$$

$$Z_n = \sqrt{R^2 + (nX_L)^2} \qquad \theta_n = \tan^{-1}\left(\frac{nX_L}{R}\right)$$

The line-to-neutral voltages, Equations (35) to (37), and the line current, Equation (38) are plotted as shown in Figure 11.

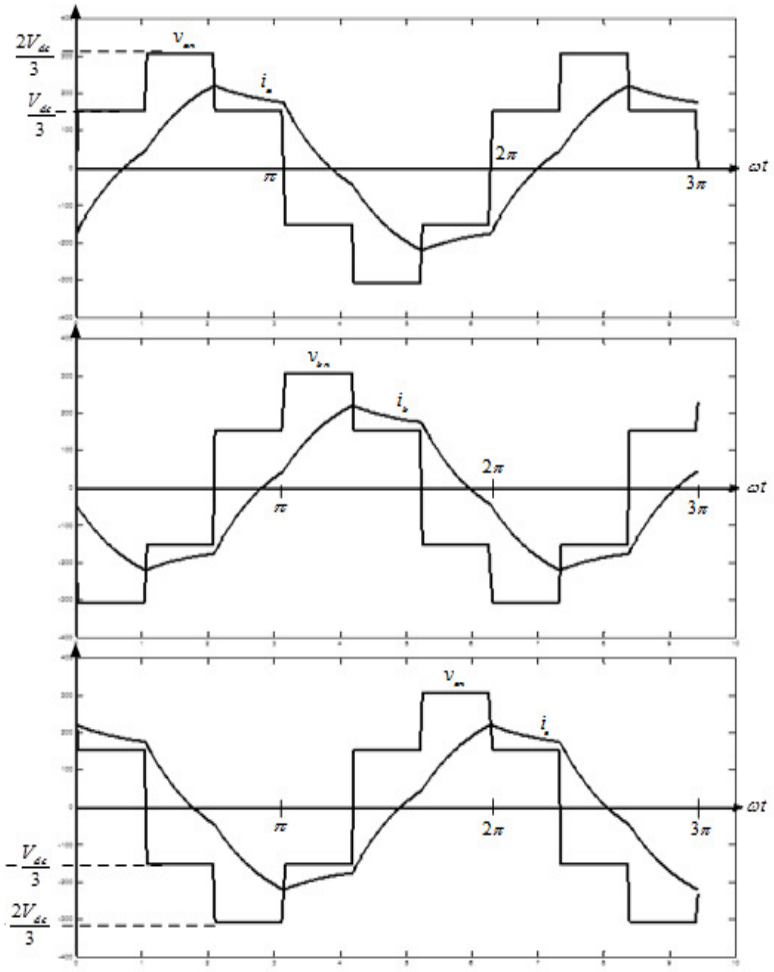

Figure 11: Phase voltages and currents

The line-to-neutral voltages of Figure 9 and Figure 11 are similar. It can be observed that a line-to-neutral voltage waveform has six steps in a cycle. Hence the name six-step inverter is used to describe this inverter. The phase "a" voltage, v_{an} - Equations (35) and current, i_a – Equation (38) are shown in Figure 12. The THD of i_a is given as:

$$THD = \left[\left(\frac{I_s}{I_{s1}}\right)^2 - 1\right]^{\frac{1}{2}} = \left[\left(\frac{10434}{10388}\right) - 1\right]^{\frac{1}{2}} = 0.0665 = 6.65\%$$

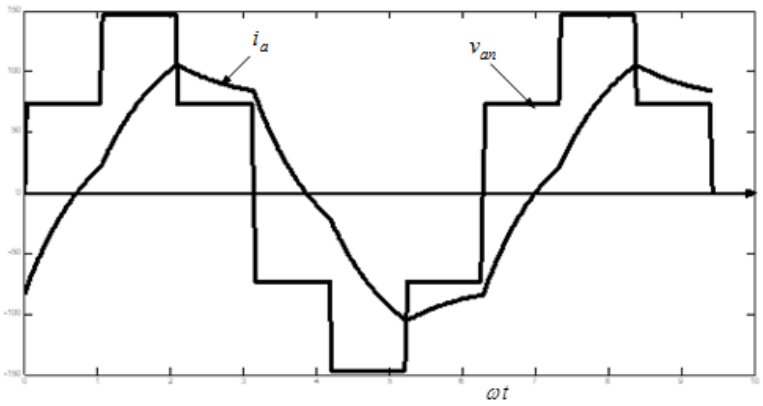

Figure 12: Phase-*a* voltage and current

3.2. Harmonics Filtering

The current of Figure 12 is distorted. Of course, we intend to achieve harmonic-free current output with the inverter. So in Figure 13 filter capacitors have been added to the inverter so as to remove the harmonics. This is the inverter topology used as active filter.

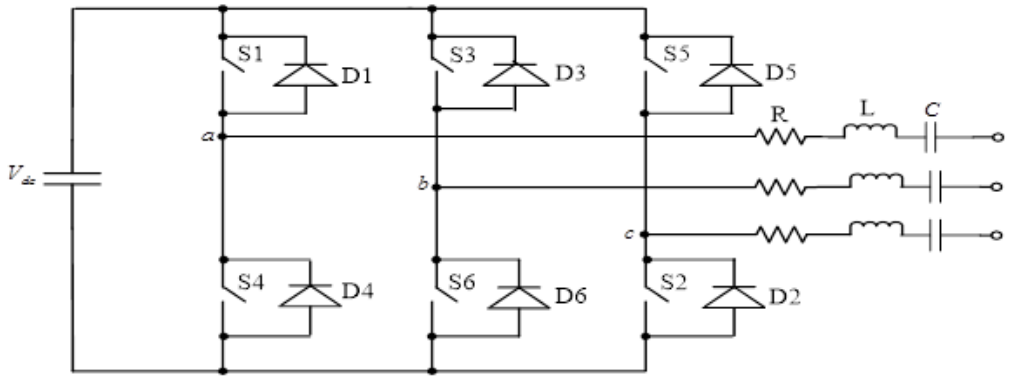

Figure 13 shows the three-phase inverter used as active filter

Appropriate values of the capacitor, inductor, resistor, and the inverter input voltage were chosen to generate sinusoidal, harmonic-free output current known as compensating current, i_c shown in Figure 14. So, the inverter produced sinusoidal, harmonic-free current output with the following circuit parameters: V_{dc} =220 V, R =1.3 Ω, L = 40 mH, C=180 µF.

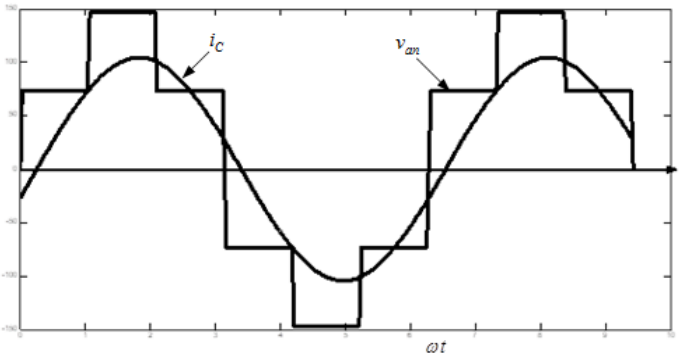

Figure 14: Output current of AF

The output sinusoidal current (Figure 14) of the active filter and the rectifier input current (i_S in Figure 5) are shown together in Figure 15. In Figure 2 we showed these currents combining to form the new input current (load current, i_L) of the rectifier (the non-linear load). The sinusoidal current from the active filter serves as compensating current (i_C) to cancel out some of the harmonics produced by the rectifier.

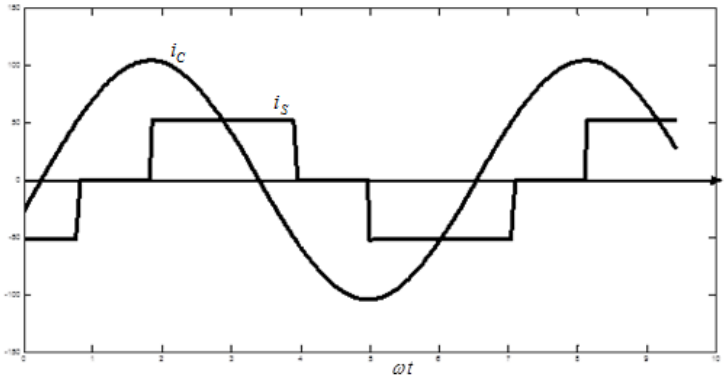

Figure 15 AF output current (i_C) and rectifier input current (i_S)

Thus, both currents in Figure 15 combine (i.e. $i_S + i_C$) in order to reduce the current harmonics present in the rectifier input current, and the result of the combination is shown in Figure 16. Thus, after compensation, the rectifier input current becomes i_L $(i_L = i_S + i_C)$. This is the compensated current with much less harmonics than the original rectifier input current (i_S).

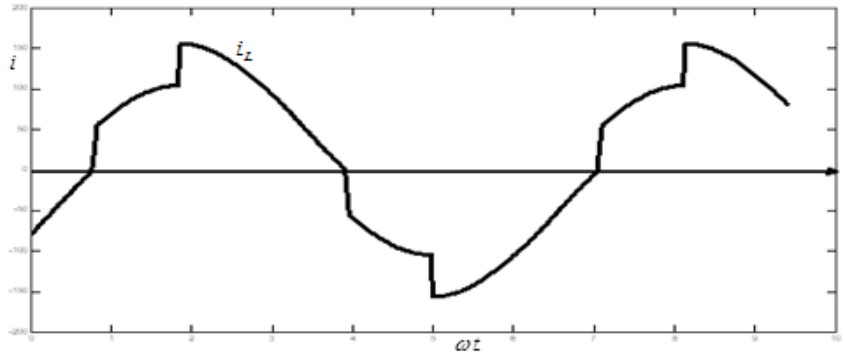

Figure 16: Rectifier compensated input current (load current, i_L)

The THD of i_L is:

$$THD = \left[\left(\frac{I_s}{I_{s1}}\right)^2 - 1\right]^{\frac{1}{2}} = \left[\left(\frac{14461}{14143}\right) - 1\right]^{\frac{1}{2}} = 0.1499 = 15\%$$

Figure 17 shows the compensated rectifier input current $i_{L,}$ its fundamental component, i_{L1} and the input voltage, $v_{S.}$ It can be observed in Figure 17 that the angle between v_S and i_{L1} is equal to 36º, i.e. power factor angle, $\theta_1 = 36^o$. Thus, the power factor of the compensated system is given by:

$$PF = \frac{I_{s1}}{I_s}\cos\theta_1 = \frac{118.924}{120.254}x\cos 36^o = 0.8$$

So the THD of rectifier input current has dropped from 31.06 % to 15 %. The system power factor now has risen from 0.25 to 0.8.

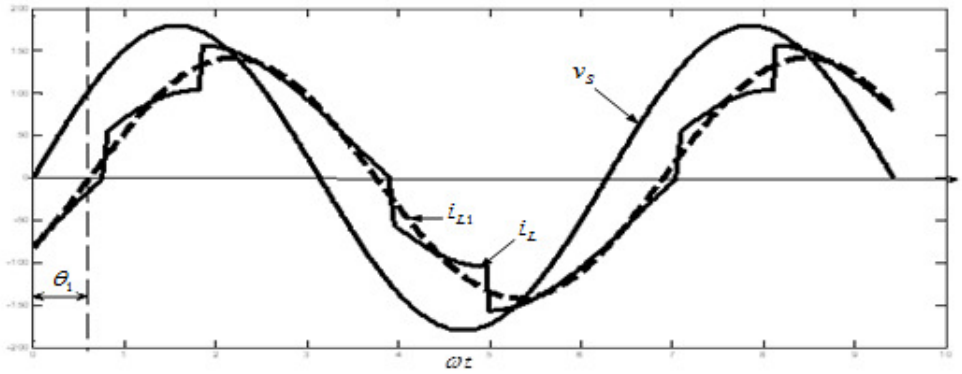

Figure 17: Compensated rectifier input current i_L , i_{L1} and input voltage v_S

4. CONCLUSION

Nonlinear loads draw harmonic and reactive power components of current from AC mains. The effects of harmonics and reactive power flow in ac systems are quite undesirable. Hence passive L-C filters were employed to reduce harmonics and capacitors were applied to improve the power factor of the ac loads. Passive filters have the disadvantages of bulkiness, resonance and fixed compensation. Therefore, the

increased severity of harmonic pollution in power networks has led to the development of the equipment known as active filters, as dynamic and adjustable solutions to the power quality problems. It has been shown in this paper that voltage-source inverter, as an active filter, can significantly minimize harmonic pollution in ac system network. The active filter reduced the THD of supply current from 31.06 % to 15 %, and raised the system power factor from 0.25 to 0.8.

5. CONFLICT OF INTEREST

There is no conflict of interest associated with this work.

REFERENCES

Allmeling, J. (2004). A control Structure for Fast Harmonics Compensation in Active Filters. *IEEE Transaction on Power Electronics,* 19, pp. 508-514.

Bose, B. K. (2000). *Modern Power Electronics and AC Drives*. Prentice Hall.

Chen, Y., Zhou, J., Dai, W. P. and Hu, E. (2014). Application of Improved Bridgeless Power Factor Correction based on one-cycle control in Electric Vehicle Charging System. *Electric Power Systems and Components*, 42(2), pp. 112-123.

Chung-Ming, Y., Sheng-Feng, W., Wei-Shan, Y. and Cheng-Wei, Y. (2014). A DC-Side Current Injection Method for Improving AC Line Condition Applied in the 18-Pulse Converter System. *IEEE Transaction on Power Electronics*, 29(1), pp. 99-109.

Dubey, G. K. (1989). *Power Semiconductor Controlled Drives*. Englewood N.J.: Prentice Hall, pp. 72-75

Emanuel, A. E. and Yang, M. (1993). On the Harmonic Compensation in non-sinusoidal Systems. *IEEE Transactions on Power Delivery,* 8, pp. 393-399.

Fitzgerald, A. E., Kingsley, C. and Umans, S. D. (2003). *Electric Machinery*. 6 Ed., New York: McGraw-Hill, pp. 524-533.

Katic, V. A. and Graovac, D. (2002). A Method for PWM Rectifier Line Side Filter Optimization in Transient and Steady State. *IEEE Transaction on Power Electronics*, 17(3), pp. 342-352

Maheshwari, R., Munk-Nielsen, S. and Lu, K. (2013). An active damping technique for small DC-link capacitor based drive system. *IEEE Transactions Industrial Information*, 9(2), pp. 848-858.

Marafao, J. A. G., Pomilio, J. A. and Spiazzi, G. (2004). Improved Three-Phase High-Quality Rectifier with Line-Commutated Switches. *IEEE Transaction on Power Electronics*, 19, pp. 640-648.

Nastran, J., Cajhen, R., Seliger, M. and Jereb, P. (1994). Active Power Filters for Nonlinear AC loads. *IEEE Transactions Power Electronics*, 9, pp. 92-96

Qiao, C and Smeldley, K. M. (2002). A General Three-phase PFC Controller for Rectifiers with Parallel-Connected Dual Boost Topology. *IEEE Transactions on Power Electronics*, 17(6), pp. 925-934.

Rashid, M. H. (1993). *Power Electronics: Circuits, Devices, and Applications*. Prentice Hall Inc., pp. 158-164.

Rim, G. H., Kang, Y., Kim, W. H., Kim, J. S. (1995). Performance improvement of a voltage source active filter. In: Proceedings of the IEEE APEC'95.

Singh, B., Al-Haddad, K. and Chandra, A. (1999). A Review of Active Filters for Power Quality Improvement. *IEEE Transactions on Industrial Electronics*, 46(5), pp. 960-972.

Srianthumrong, S., Fujita, H. and Akagi, H. (2002). Stability Analysis of a Series Active Filter Integrated with Double-Series Diode Rectifier. *IEEE Transaction on Power Electronics*, 17(1), pp. 117-124.